




Thermodynamic properties of calcium alkali phosphates $\text{Ca}(\text{Na},\text{K})\text{PO}_4$

Hannes Herzel^{1,*} , Klaus-Dieter Grevel², Franziska Emmerling¹, Edgar Dachs³, Artur Benisek³, Christian Adam¹, and Juraj Majzlan²

¹Bundesanstalt für Materialforschung und -prüfung (BAM), Unter den Eichen 87, 12205 Berlin, Germany

²Institute of Geosciences, Friedrich-Schiller University, Burgweg 11, 07749 Jena, Germany

³Department of Chemistry and Physics of Materials, University of Salzburg, Jakob-Haringer-Strasse 2a, 5020 Salzburg, Austria

Received: 12 February 2020

Accepted: 26 March 2020

Published online:

12 April 2020

© The Author(s) 2020

ABSTRACT

Calcium alkali phosphates $\text{Ca}(\text{Na},\text{K})\text{PO}_4$ are main constituents of bioceramics and thermochemically produced phosphorus fertilizers because of their bioavailability. Sparse thermodynamic data are available for the endmembers CaNaPO_4 and CaKPO_4 . In this work, the missing data were determined for the low-temperature phase modifications of the endmembers CaNaPO_4 and CaKPO_4 and three intermediate $\text{Ca}(\text{Na},\text{K})\text{PO}_4$ compositions. Standard enthalpy of formation ranges from $-2018.3 \pm 2.2 \text{ kJ mol}^{-1}$ to $-2030.5 \pm 2.1 \text{ kJ mol}^{-1}$ and standard entropy from $137.2 \pm 1.0 \text{ J mol}^{-1} \text{ K}^{-1}$ to $148.6 \pm 1.0 \text{ J mol}^{-1} \text{ K}^{-1}$ from sodium endmember $\beta\text{-CaNaPO}_4$ to potassium endmember $\beta'\text{-CaKPO}_4$. Thermodynamic functions are calculated up to 1400 K for endmembers and the sodium-rich intermediate phase $\beta\text{-Ca}(\text{Na}_{0.93}\text{K}_{0.07})\text{PO}_4$. Functions above 640 K are extrapolated because of the phase transition from low- to high-temperature phase. Impurities in the synthesized intermediate phases $\gamma\text{-Ca}(\text{Na}_{0.4}\text{K}_{0.6})\text{PO}_4$ and $\gamma\text{-Ca}(\text{Na}_{0.35}\text{K}_{0.65})\text{PO}_4$ and one additional phase transition around 500 K impeded the determination of high-temperature thermodynamic functions. In general, data for phase transition temperatures agree with the previously reported phase diagrams.

Introduction

Calcium alkali phosphates $\text{Ca}(\text{Na},\text{K})\text{PO}_4$ are of interest for fertilizer production and bioceramics used for bone tissue reconstructions. They possess higher bioavailability in comparison to the calcium phosphates such as whitlockite or apatite [1]. If used

as bone substitution, they should be slowly decomposed and gradually replaced by a new fully functional bone [2, 3]. For the use as fertilizers, the nutrient elements should be available to plants. Therefore, calcium alkali phosphates are produced by thermochemical treatment of rock phosphate or sewage sludge ash at 800–1400 °C with alkali sulfates, carbonates or hydroxides [4–6].

Address correspondence to E-mail: herzelhannes@gmail.com

The earliest description of CaNaPO_4 and CaKPO_4 dates back to the time of the development of the Rhenania process for thermochemical treatment of rock phosphate in the 1920s [6, 7] and the research continues until today [4, 8, 9]. Based on these procedures, a comparable thermochemical process was developed to treat phosphorus-rich sewage sludge ash for fertilizer production [5, 10, 11].

The phase diagram of the system CaNaPO_4 – CaKPO_4 was investigated by Orlov et al. [12] and Znamierowska [13] (Fig. 1). The transformation temperatures from the low- to the high-temperature modification of calcium alkali phosphates are in the range of 823 K to 1033 K. The low-temperature modifications are divided by two miscibility gaps into three stability fields (β -, β' - and γ -phase) [13]. The sodium-rich β -phase includes the chemical composition ranging from CaNaPO_4 to $\text{Ca}(\text{Na}_{0.8}\text{K}_{0.2})\text{PO}_4$ and the potassium-rich β' -phase that from CaKPO_4 to $\text{Ca}(\text{Na}_{0.05}\text{K}_{0.95})\text{PO}_4$. The intermediate γ -phase, with a composition centered around $\text{Ca}(\text{Na}_{0.5}\text{K}_{0.5})\text{PO}_4$ to $\text{Ca}(\text{Na}_{0.4}\text{K}_{0.6})\text{PO}_4$, is a target phase for bioceramic applications [14, 15]. The endmember CaNaPO_4 was intensively characterized [12, 16–18], whereas CaKPO_4 was investigated less [12, 18, 19].

Incomplete thermodynamic data are available for the endmembers CaNaPO_4 and CaKPO_4 as well as for the intermediate phase $\text{Ca}(\text{Na}_{0.4}\text{K}_{0.6})\text{PO}_4$. The transition enthalpy from the low- to the high-temperature modification ($\Delta_{\text{trans}}H$) of CaNaPO_4 , $\text{Ca}(\text{Na}_{0.4}\text{K}_{0.6})\text{PO}_4$ and CaKPO_4 is 8.2, 1.4 and 2.8 kJ mol^{-1} , respectively [12]. The database of FactSage, without citing data sources or specifying low-

and high-temperature modifications, contains the standard entropy of $128.7 \text{ J mol}^{-1} \text{ K}^{-1}$ and enthalpy of formation of $-2033 \text{ kJ mol}^{-1}$ for CaNaPO_4 . The enthalpy of formation for CaKPO_4 is calculated as $-2037.8 \text{ kJ mol}^{-1}$ [20]. To the best of our knowledge, there are no thermodynamic data for the potassium and sodium-containing intermediate calcium alkali phosphates. To close some of these gaps, this work presents heat capacity, standard entropy and standard enthalpy of formation for the endmembers β - CaNaPO_4 and β' - CaKPO_4 as well as for three intermediate phases.

Experimental methods

Synthesis

Low-temperature modifications of each calcium alkali phosphate $\text{Ca}(\text{Na,K})\text{PO}_4$ were synthesized using protocols that avoid the use of excessive heat in order to remain well below the transformation temperature to the high-temperature modification. Other syntheses, e.g. β - CaNaPO_4 by Morris et al. [21] and Ben Amara et al. [16], $\text{Ca}_2\text{NaK}(\text{PO}_4)_2$ by Schneider et al. [14] and β - CaKPO_4 by Franck et al. [22], include steps above the transformation temperatures. The syntheses of β - CaNaPO_4 and the sodium-rich intermediate phase β - $\text{Ca}(\text{Na}_{0.93}\text{K}_{0.07})\text{PO}_4$ completely below the transformation temperature are only possible if all chemicals can be initially dissolved in water and thoroughly mixed. Thus, stoichiometric mixtures of $\text{Ca}(\text{NO}_3)_2 \cdot 2\text{H}_2\text{O}$, H_3PO_4 , NaNO_3 and KNO_3 (all p.a. grade) were completely dissolved in double-distilled water. The solution was treated at first at 383 K to evaporate the water and subsequently the powder at 573 K for 3 h in a muffle furnace to remove NO_x . The dry material was ground in a vibrating tungsten-carbide cup mill (Pulverisette, Siebtechnik). The sintering process at 773 K was interrupted by grinding and re-grinding after 12, 24, 48, 96 and 192 h. However, β' - CaKPO_4 and the intermediate phases γ - $\text{Ca}(\text{Na}_{0.4}\text{K}_{0.6})\text{PO}_4$ and γ - $\text{Ca}(\text{Na}_{0.35}\text{K}_{0.65})\text{PO}_4$ could not be synthesized in a pure form using this protocol. Therefore, the syntheses of intermediate phases and β' - CaKPO_4 were modified and combined with the protocol of Schneider et al. [14]. The chemicals $\text{CaHPO}_4 \cdot 2\text{H}_2\text{O}$, Na_2CO_3 and K_2CO_3 (all p.a. grade) were thoroughly mixed and heated to 1173 K for 1 h. Afterwards they were

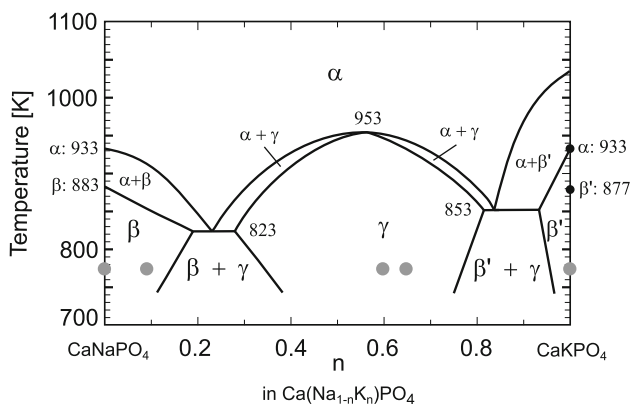


Figure 1 Phase diagram of CaNaPO_4 – CaKPO_4 simplified after Znamierowska [13]. The grey circles represent investigated five samples at their preparation temperature 773 K. Pure CaKPO_4 has phase transitions at 877 K and 933 K.

ground, sintered at 773 K with interruption of re-grinding after 12, 24, 48, 96 and 192 h, as described for the β -phases. Additionally, α -CaKPO₄ was prepared with the same chemicals as β' -CaKPO₄ but heated to 1273 K for 6 h. Afterwards, this sample was quenched in water.

Sample characterization

Chemical analysis

The chemical composition was analysed by inductively coupled plasma mass spectrometry (ICP-MS; Thermo iCAP Q, Dreieich, Germany) after digestion with aqua regia (chemicals p.a. grade) of 0.05–0.1 g sample in a microwave. Blanks, KCl (p.a. grade), NaCl (p.a. grade) and a reference material D826-1 for Ca and P were used to evaluate the analytical accuracy and precision. All digestions and ICP-MS measurements were carried out in triplicates.

Powder X-ray diffraction (PXRD)

PXRD measurements of the samples were performed in transmission geometry over a 2θ range from 5° to 70°, with a step size of 0.0009° (D8 Discover, Bruker AXS) and with Cu K α_1 ($\lambda = 1.54056 \text{ \AA}$) radiation. The diffraction patterns were recorded with a Lynxeye detector. The PXRD were evaluated using the Match! Software (version 3.6). Full-profile refinements were done for the samples β -CaNaPO₄ and β -Ca(Na_{0.93}-K_{0.07})PO₄ (TOPAS version 6). The content of impurities was estimated additionally by the area method. This method is more closely described in the supplementary information.

Calorimetry

Acid-solution calorimetry

For the solution calorimetric experiments at $T = 298.15 \text{ K}$, we used a commercial IMC-4400 isothermal microcalorimeter (Calorimetry Sciences Corporation), modified for the purposes of acid-solution calorimetry [23]. The liquid bath of the calorimeter was held at a constant temperature of 298.15 K with fluctuations smaller than 0.0005 K. The calorimetric solvent was 25 g of 5 N HCl contained in a polyetheretherketone (PEEK) cup with a total volume of 60 mL. The cup was then closed with a PEEK

screwable lid and inserted into the calorimeter well. The calorimeter stabilized after $\approx 8 \text{ h}$. During the stabilization and the experiment, the solvent was stirred by a SiO₂ glass stirrer by a motor positioned about 40 cm from the active zone of the instrument. The samples were pressed into a pellet and weighed on a micro-balance with a precision of 0.002 mg (as stated by the manufacturer). The pellets were then dropped through a SiO₂ glass tube into the solvent and the heat produced or consumed during the dissolution was measured. The heat flow between the reaction cup and the constant temperature reservoir was then integrated to calculate the caloric effect. A typical experiment lasted 70–80 min and the end of the experiment was judged from the return of the baseline to the pre-experiment position. The calorimeter was calibrated by dissolving $\approx 20 \text{ mg}$ pellets of KCl in 25 g of deionized water. Prior to each calibration measurement, the potassium chloride was heated overnight in the furnace to 800 K to remove the adsorbed water. The expected heat effect for the calibration runs was calculated from Parker [24].

Relaxation calorimetry (PPMS)

Heat capacity (C_p) was measured by relaxation calorimetry using a commercial Physical Properties Measurement System (PPMS, from Quantum Design, San Diego, California). With due care, accuracy can be within 1% for 5 K to 300 K, and 5% for 0.7 K to 5 K [25]. Powdered samples were wrapped in a thin Al foil and compressed to produce a $\approx 0.5 \text{ mm}$ thick pellet which was then placed onto the sample platform of the calorimeter for measurement. Heat capacity was measured in the PPMS in the temperature interval 2 K to 300 K.

Differential scanning calorimetry (DSC and STA)

The heat capacities between 259 and 640 K for sample β -CaNaPO₄ and 282 K and 464 K for other samples were measured by differential scanning calorimetry (DSC) using a Perkin Elmer Diamond DSC. Details of the method are described in Benisek et al. [26].

C_p measurements at 310–1370 K were done with a Netzsch STA 449 C Jupiter thermoanalytical system (STA). The sample was loaded into platinum crucibles covered by platinum lids. Accuracy was regularly tested by the determination of C_p of sapphire.

Accuracy of transformation enthalpy ($\Delta_{\text{trans}}H$) measurements was tested by measurements on quartz, SiO_2 . The measured $\Delta_{\text{trans}}H$ of $0.543 \pm 0.007 \text{ kJ mol}^{-1}$ (in duplicate) compares roughly to the $0.625 \text{ kJ mol}^{-1}$ from Hemingway [27], the deviation being 13%.

Results and discussion

Chemical and phase characterization

The chemical compositions of the synthesis products were determined by ICP-MS and compared to the nominal elemental mass fractions calculated from the ratios of the starting chemicals (Table 1). The accuracies for calcium and phosphorus were between 97 and 103 wt% compared to the expected values and for sodium and potassium slightly below 100 wt% for all samples. Chemical analysis by ICP-MS was confirmed by X-ray fluorescence spectroscopy (data not shown).

All samples were crystalline, with sharp PXRD peaks. The models for the sample $\beta\text{-CaNaPO}_4$ (space group $Pn2_1a$; $a = 20.3806(3) \text{ \AA}$; $b = 5.40518(9) \text{ \AA}$; $c = 9.1562(2) \text{ \AA}$; $V = 1008.6(1) \text{ \AA}^3$) and the sample $\beta\text{-Ca}(\text{Na}_{0.93}\text{K}_{0.07})\text{PO}_4$ ($Pn2_1a$; $a = 20.4633(9) \text{ \AA}$; $b = 5.4124(2) \text{ \AA}$; $c = 9.1771(4) \text{ \AA}$; $v = 1016.4(1) \text{ \AA}^3$) were refined by using ICSD entry 35629 (supplementary Fig. S1 and S2). The indexing of the diffraction pattern of $\beta\text{-Ca}(\text{Na}_{0.93}\text{K}_{0.07})\text{PO}_4$ documents expansion of the unit cell in comparison to $\beta\text{-CaNaPO}_4$, because of incorporation of the larger K atoms in its structure. Furthermore, there are additional $\text{CaK}_2\text{P}_2\text{O}_7$ reflexes in the PXRD data for the sample $\beta\text{-Ca}(\text{Na}_{0.93}\text{K}_{0.07})\text{PO}_4$ (Fig. S2). The amount of $\text{CaK}_2\text{P}_2\text{O}_7$ (COD entry 9007955) was quantified by

Rietveld refinement as 3 wt%. Application of the semiquantitative area method yielded 4 wt% (see supplementary information). Combined with the results of chemical analysis, the assumed composition of this sample is 96 wt% $\beta\text{-Ca}(\text{Na}_{0.93}\text{K}_{0.07})\text{PO}_4$ and 4 wt% $\text{CaK}_2\text{P}_2\text{O}_7$.

The PXRD peaks of the two samples of $\gamma\text{-Ca}(\text{Na}_{0.4}\text{K}_{0.6})\text{PO}_4$ and $\gamma\text{-Ca}(\text{Na}_{0.35}\text{K}_{0.65})\text{PO}_4$ are slightly shifted to lower 2θ angles compared to the data entry $\text{Ca}_2\text{NaK}(\text{PO}_4)_2$ (ICDD PDF entry 00-051-0579) (Fig. S3). Furthermore, similar refinement is achieved with lattice parameters for a monoclinic system postulated for $\text{Ca}(\text{Na}_{0.4}\text{K}_{0.6})\text{PO}_4$ by Orlov et al. [12]. Both samples contain impurities but the quantification of these impurities by Rietveld refinement was not possible, because a structural model for $\text{Ca}_2\text{NaK}(\text{PO}_4)_2$ [14] or $\text{Ca}(\text{Na}_{0.4}\text{K}_{0.6})\text{PO}_4$ [12] is not available. Therefore, the content of impurities was estimated by the area method. Accordingly, $\gamma\text{-Ca}(\text{Na}_{0.4}\text{K}_{0.6})\text{PO}_4$ contains 5 wt% whitlockite (ICSD entry 91525), 1 wt% $\text{CaK}_2\text{P}_2\text{O}_7$, and 0.5 wt% hydroxylapatite ($\text{Ca}_5(\text{PO}_4)_3\text{OH}$) (COD entry 9011095). $\gamma\text{-Ca}(\text{Na}_{0.35}\text{K}_{0.65})\text{PO}_4$ contains 2 wt% hydroxylapatite as an impurity.

There are very few structural data for the low-temperature phase $\beta'\text{-CaKPO}_4$. Our data could be refined with lattice parameters $a = 5.492(4) \text{ \AA}$; $b = 9.603(2) \text{ \AA}$; $c = 16.245(5) \text{ \AA}$; $\beta = 68.9(1)$; $V = 799.6(4) \text{ \AA}^3$ from Orlov et al. [12]. Evdokimov et al. [3] described this phase as “a monoclinic distortion of the hexagonal structure of $\alpha\text{-CaKPO}_4$ ” and, therefore, the reflexes of $\beta'\text{-CaKPO}_4$ coincide largely with those of $\alpha\text{-CaKPO}_4$ (Fig. S4). The sample $\beta'\text{-CaKPO}_4$ contains 2 wt% $\text{CaK}_2\text{P}_2\text{O}_7$, 3 wt%

Table 1 Chemical composition of calcium alkali phosphates $\text{Ca}(\text{Na,K})\text{PO}_4$, measured in triplicates.

Chemical composition is normalized to the molar proportions to 1 P atom per formula unit in the row below the mass fraction

Sample	Mass fraction [wt%]			
	Ca	K	Na	P
$\beta\text{-CaNaPO}_4$	24.59 ± 0.34	–	13.55 ± 0.01	19.03 ± 0.17
	1.00	–	0.96	1.00
$\beta\text{-Ca}(\text{Na}_{0.93}\text{K}_{0.07})\text{PO}_4$	24.85 ± 1.61	2.51 ± 0.37	12.21 ± 0.16	19.29 ± 1.03
	1.00	0.10	0.85	1.00
$\gamma\text{-Ca}(\text{Na}_{0.4}\text{K}_{0.6})\text{PO}_4$	24.46 ± 0.27	13.25 ± 0.02	5.26 ± 0.01	18.10 ± 0.13
	1.04	0.58	0.39	1.00
$\gamma\text{-Ca}(\text{Na}_{0.35}\text{K}_{0.65})\text{PO}_4$	23.97 ± 0.28	14.05 ± 0.16	4.61 ± 0.02	17.70 ± 0.08
	1.05	0.63	0.35	1.00
$\beta'\text{-CaKPO}_4$	23.63 ± 0.21	20.06 ± 0.01	–	17.35 ± 0.20
	1.05	0.92	–	1.00

whitlockite and 3 wt% hydroxylapatite as impurities, estimated with the area method.

Acid-solution calorimetry

The enthalpies of formation of calcium alkali phosphates $\text{Ca}(\text{Na,K})\text{PO}_4$ were determined by acid-solution calorimetry. All samples and reference compounds dissolved rapidly, and the results were reproducible, with uncertainties typical for this type of measurements. The measured bulk enthalpies in 5 N HCl are weighed sums of the enthalpies of dissolution ($\Delta_{\text{diss}}H$) of the $\text{Ca}(\text{Na,K})\text{PO}_4$ phase and the impurities. To evaluate and correct for the latter, we also measured $\Delta_{\text{diss}}H$ for K-whitlockite [$\text{Ca}_{10}\text{K}(\text{PO}_4)_7$] as $336.7 \pm 0.3 \text{ kJ mol}^{-1}$ and $\Delta_{\text{diss}}H$ for hydroxylapatite [$\text{Ca}_5(\text{PO}_4)_3\text{OH}$] as $-124.3 \text{ kJ mol}^{-1}$. The $\Delta_{\text{diss}}H$ for $\text{CaK}_2\text{P}_2\text{O}_7$ was not measured but calculated from enthalpy of formation of $\text{CaK}_2\text{P}_2\text{O}_7$ of $-3286.9 \text{ kJ mol}^{-1}$ from Zdukos et al. [20]. The calculated value is $-69.4 \text{ kJ mol}^{-1}$. $\Delta_{\text{diss}}H$ of the impurities were used to correct the bulk $\Delta_{\text{diss}}H$ values in order to achieve the $\Delta_{\text{diss}}H$ values for pure calcium alkali phosphates.

The corrected $\Delta_{\text{diss}}H$ in 5 N HCl decreases monotonically with increasing potassium content in the $\text{Ca}(\text{Na}_{1-n}\text{K}_n)\text{PO}_4$ solid solution from $-52.23 \pm 0.30 \text{ kJ mol}^{-1}$ for sample $\beta\text{-CaNaPO}_4$ to $-62.69 \pm 0.14 \text{ kJ mol}^{-1}$ for the sample $\beta'\text{-CaKPO}_4$ (Table 3). The corrected $\Delta_{\text{diss}}H$ are used to calculate deviations of the intermediate phases $\text{Ca}(\text{Na}_{1-n}\text{K}_n)\text{PO}_4$ from the enthalpy of theoretical mixtures of the endmembers (Fig. 2). This calculation is comparable to the determination of enthalpy of mixing [28].

The enthalpy of formation from elements in their standard state has to be calculated via a thermochemical cycle (Table 2) with respect to the known enthalpies of carefully chosen substances called the reference compounds. Special attention should be given to these reference compounds. Their formation enthalpies must be known with high accuracy and precision.

The thermochemical cycles were constructed with KH_2PO_4 , $\text{NaH}_2\text{PO}_4 \cdot 2\text{H}_2\text{O}$, CaO and H_2O as the reference compounds (Table 2). The $\Delta_{\text{diss}}H$ of CaO was reported by Majzlan [23]. The dissolution enthalpy of KH_2PO_4 in 5 N HCl at $T = 298 \text{ K}$ at low final molalities was measured as $24.61 \pm 0.46 \text{ kJ mol}^{-1}$ [29]. In our study, the $\Delta_{\text{diss}}H$ of $25.08 \pm 0.28 \text{ kJ mol}^{-1}$ was measured for higher final molalities. The dissolution

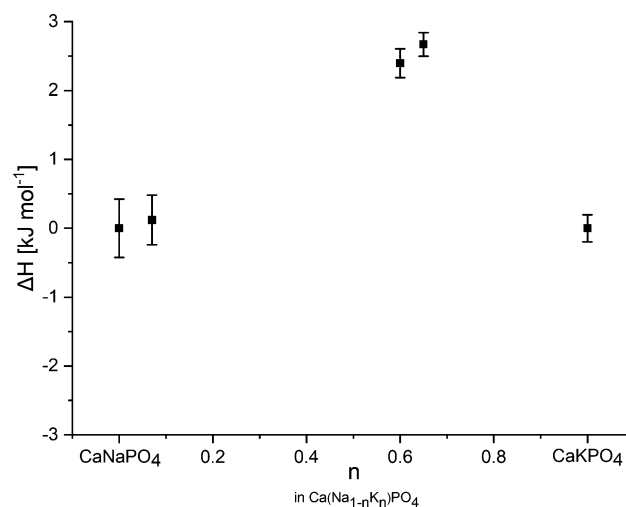


Figure 2 Deviation (ΔH) of experimental $\Delta_{\text{diss}}H$ of synthesized $\text{Ca}(\text{Na}_{1-n}\text{K}_n)\text{PO}_4$ from calculated $\Delta_{\text{diss}}H$ for theoretical mixtures of $\beta\text{-CaNaPO}_4$ and $\beta'\text{-CaKPO}_4$.

enthalpy of $\text{NaH}_2\text{PO}_4 \cdot 2\text{H}_2\text{O}$ in 5 N HCl at $T = 298 \text{ K}$ was measured in our study as $29.83 \pm 0.32 \text{ kJ mol}^{-1}$; no data are available in the literature for comparison.

There are only few data for the formation enthalpies of the phosphates KH_2PO_4 and $\text{NaH}_2\text{PO}_4 \cdot 2\text{H}_2\text{O}$. The formation enthalpy of KH_2PO_4 can be found in Rud'ko et al. ([30]; $-1561.9 \text{ kJ mol}^{-1}$), Wagman et al. ([31]; $-1586.3 \text{ kJ mol}^{-1}$), and Luff and Reed ([32]; $-1573.6 \text{ kJ mol}^{-1}$). Majzlan [23] re-determined the formation enthalpy of KH_2PO_4 as $-1573.6 \text{ kJ mol}^{-1}$ and adopted the value from Luff and Reed [32], as done in this paper. For $\text{NaH}_2\text{PO}_4 \cdot 2\text{H}_2\text{O}$, only the data in Wagman [31] are available and are adopted in this work.

The calculated enthalpies of formation from elements in their standard state ($\Delta_f H^\circ$) decrease with increasing potassium content from $-2018.3 \pm 2.2 \text{ kJ mol}^{-1}$ ($\beta\text{-CaNaPO}_4$) to $-2030.5 \pm 2.1 \text{ kJ mol}^{-1}$ ($\beta'\text{-CaKPO}_4$) (Table 3).

Standard entropy and Gibbs free energy of formation

Standard entropies were calculated by heat capacity data of PPMS. These data of the $\text{Ca}(\text{Na,K})\text{PO}_4$ samples in the temperature range 2 to 303 K were fitted with polynomials:

$$\sum_{N=0}^{11} A_N T^N$$

Table 2 Thermodynamic cycle for calcium-alkali-phosphates used for acid solution calorimetry

$\Delta H_1 =$	$\Delta_{\text{diss}}H(\text{CaNa}_{(1-n)}\text{K}_n\text{PO}_4)$	$\text{CaNa}_{(1-n)}\text{K}_n\text{PO}_4 (\text{cr}) \rightarrow \text{Ca}^{2+} (\text{aq}) + (1-n) \text{Na}^+ (\text{aq}) + n \text{K}^+ (\text{aq}) + \text{PO}_4^{3-} (\text{aq})$	see Table 3
$\Delta H_2 =$	$\Delta_{\text{diss}}H(\text{NaH}_2\text{PO}_4 \cdot 2\text{H}_2\text{O})$	$\text{NaH}_2\text{PO}_4 \cdot 2\text{H}_2\text{O} (\text{cr}) \rightarrow \text{Na}^+ (\text{aq}) + 2\text{H}^+ (\text{aq}) + \text{PO}_4^{3-} (\text{aq}) + 2 \text{H}_2\text{O} (\text{aq})$	$29.83^{\text{a}} \pm 0.32^{\text{b}} (4)^{\text{c}}$
$\Delta H_3 =$	$\Delta_{\text{diss}}H(\text{KH}_2\text{PO}_4)$	$\text{KH}_2\text{PO}_4 (\text{cr}) \rightarrow \text{K}^+ (\text{aq}) + 2\text{H}^+ (\text{aq}) + \text{PO}_4^{3-} (\text{aq})$	$25.08 \pm 0.28 (4)$
$\Delta H_4 =$	$\Delta_{\text{diss}}H(\text{CaO})$	$\text{CaO} (\text{cr}) + 2\text{H}^+ \rightarrow \text{Ca}^{2+} (\text{aq}) + \text{H}_2\text{O} (\text{aq})$	$-195.86 \pm 1.64^{\text{d}}$
$\Delta H_5 =$	$\Delta_{\text{dilution}}H(\text{H}_2\text{O})$	$\text{H}_2\text{O} (\text{l}) \rightarrow \text{H}_2\text{O} (\text{aq})$	-0.54^{e}
$\Delta H_6 =$	$\Delta_f H^\circ(\text{NaH}_2\text{PO}_4 \cdot 2\text{H}_2\text{O})$	$\text{Na} (\text{cr}) + 3 \text{H}_2 (\text{g}) + \text{P} (\text{cr}) + 3 \text{O}_2 (\text{g}) \rightarrow \text{NaH}_2\text{PO}_4 \cdot 2\text{H}_2\text{O} (\text{cr})$	$-2128.4 \pm 1.0^{\text{f,g}}$
$\Delta H_7 =$	$\Delta_f H^\circ(\text{KH}_2\text{PO}_4)$	$\text{K} (\text{cr}) + \text{H}_2 (\text{g}) + \text{P} (\text{cr}) + 2 \text{O}_2 (\text{g}) \rightarrow \text{KH}_2\text{PO}_4 (\text{cr})$	$-1573.6 \pm 1.0^{\text{h,g}}$
$\Delta H_8 =$	$\Delta_f H^\circ(\text{CaO})$	$\text{Ca} (\text{cr}) + 1/2 \text{O}_2 (\text{g}) \rightarrow \text{CaO} (\text{cr})$	$-635.1 \pm 0.9^{\text{i}}$
$\Delta H_9 =$	$\Delta_f H^\circ(\text{H}_2\text{O})$	$\text{H}_2 (\text{g}) + 1/2 \text{O}_2 (\text{g}) \rightarrow \text{H}_2\text{O} (\text{l})$	$-285.8 \pm 0.1^{\text{i}}$
$\Delta H_{10} =$	$\Delta_f H^\circ(\text{CaNa}_{(1-n)}\text{K}_n\text{PO}_4)$	$\text{Ca} (\text{cr}) + (1-n) \text{Na} (\text{cr}) + n \text{K} (\text{cr}) + \text{P} (\text{cr}) + 2 \text{O}_2 (\text{g}) \rightarrow \text{CaNa}_{(1-n)}\text{K}_n\text{PO}_4 (\text{cr})$	
$\Delta H_{10} =$	$\Delta_f H^\circ(\text{CaNa}_{(1-n)}\text{K}_n\text{PO}_4) =$	$-\Delta H_1 + (1-n) \Delta H_2 + n \Delta H_3 + \Delta H_4 - (3-2n) \Delta H_5 + (1-n) \Delta H_6 + n \Delta H_7 + \Delta H_8 - (3-2n) \Delta H_9$	

^aMean^bTwo standard deviations of the mean^cNumber of measurements^dMajzlan [23]^eCalculated from Parker [24]^fWagman et al. [31]^gNo uncertainty available; estimated as 1.0 kJ mol^{-1} ^hLuff and Reed [32]ⁱRobie and Hemingway [33]

Experimental data in the temperature range 2–15 K could not be fitted with a simple ($N = 3$) or extended Debye ($N = 3, 5, 7$) model. Therefore, the low-temperature data were fitted and extrapolated to 0 K with polynomials with $N = 1-7$. The physical meaning of all these terms is not clear but the achieved fits are satisfactory. The temperature range 15–300 K was subdivided in three sections (15–60 K, 60–160 K and 160–300 K) and fitted with orthogonal polynomials. All coefficients (A_N) are listed in the supplementary information. The relative deviation between experimental data and fits [28] are shown in Fig. 3 for β - CaNaPO_4 and in the supplementary information for the other phases. The integration according to these orthogonal polynomials for heat capacity was used to calculate standard entropies S° :

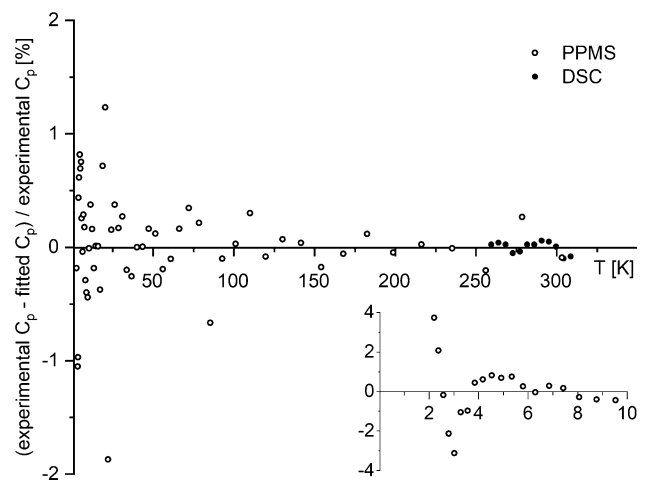


Figure 3 Deviation of experimental C_p and fitted C_p of PPMS (empty circles) against temperature for β - CaNaPO_4 . The inset shows the temperature range 2–10 K. Experimental C_p of DSC (filled circles) plotted against fitted C_p of PPMS.

$$S^\circ = \int_0^{15} \frac{F_1(T)}{T} dT + \int_{15}^{60} \frac{F_2(T)}{T} dT + \int_{60}^{160} \frac{F_3(T)}{T} dT + \int_{160}^{300} \frac{F_4(T)}{T} dT$$

The calculated standard entropies are, just as the enthalpies, weighed averages of the entropy of the $\text{Ca}(\text{Na}_{1-n}\text{K}_n)\text{PO}_4$ phases and the impurities. The S° value for hydroxyapatite of $390.4 \text{ J mol}^{-1} \text{ K}^{-1}$ was taken from Robie and Hemingway [33]. The S° values for the other impurities were estimated with the Neumann-Kopp rule, stating that the entropy of a phase is the sum of entropies of its suitably chosen components. In this case, the components are simple oxides and their entropies were taken from Robie and Hemingway [33]. The estimated entropies of K-whitlockite and $\text{CaK}_2\text{P}_2\text{O}_7$ are $828.5 \text{ J mol}^{-1} \text{ K}^{-1}$ and $246.6 \text{ J mol}^{-1} \text{ K}^{-1}$, respectively. The S° values for the $\text{Ca}(\text{Na}_{1-n}\text{K}_n)\text{PO}_4$ phases, corrected for the impurities, increase from $137.2 \pm 1.0 \text{ J mol}^{-1} \text{ K}^{-1}$ for $\beta\text{-CaNaPO}_4$ to $148.6 \pm 1.0 \text{ J mol}^{-1} \text{ K}^{-1}$ for $\beta'\text{-CaKPO}_4$ (Table 3). Their deviations from entropies of theoretical mixtures of the endmembers are displayed in Fig. 4.

The calculated Gibbs free energies of formation decrease with increasing potassium content from $-1896.5 \pm 2.4 \text{ kJ mol}^{-1}$ for $\beta\text{-CaNaPO}_4$ to $-1908.1 \pm 2.4 \text{ kJ mol}^{-1}$ for $\beta'\text{-CaKPO}_4$. The $\Delta_f G^\circ$ for $\beta\text{-CaNaPO}_4$ is 12 kJ mol^{-1} higher than that in the database of the software FactSage (Table 3).

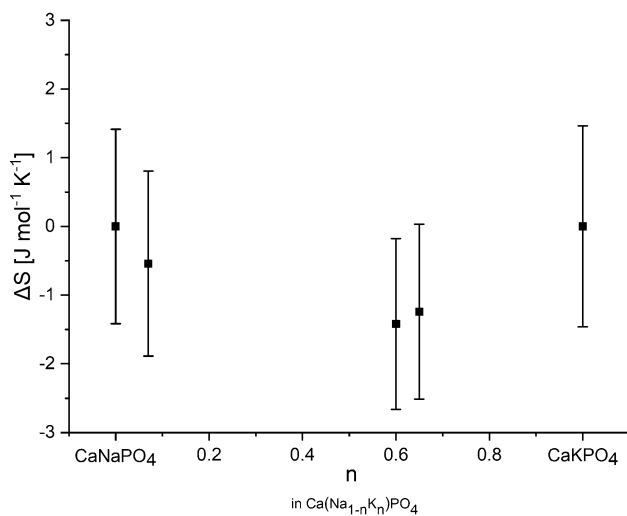


Figure 4 Deviation (ΔS) of experimental S° of synthesized $\text{Ca}(\text{Na}_{1-n}\text{K}_n)\text{PO}_4$ from calculated S° for theoretical mixtures of $\beta\text{-CaNaPO}_4$ and $\beta'\text{-CaKPO}_4$.

Table 3 Thermodynamic properties of five calcium alkali phosphates derived from calorimetric measurements based on corrected values of $\Delta_{\text{diss}}H$ and S° . Data in italics in the first row are from the modelling software FactSage [35]. All enthalpy and Gibbs free energy values in kJ mol^{-1} , all entropies in $\text{J mol}^{-1} \text{ K}^{-1}$

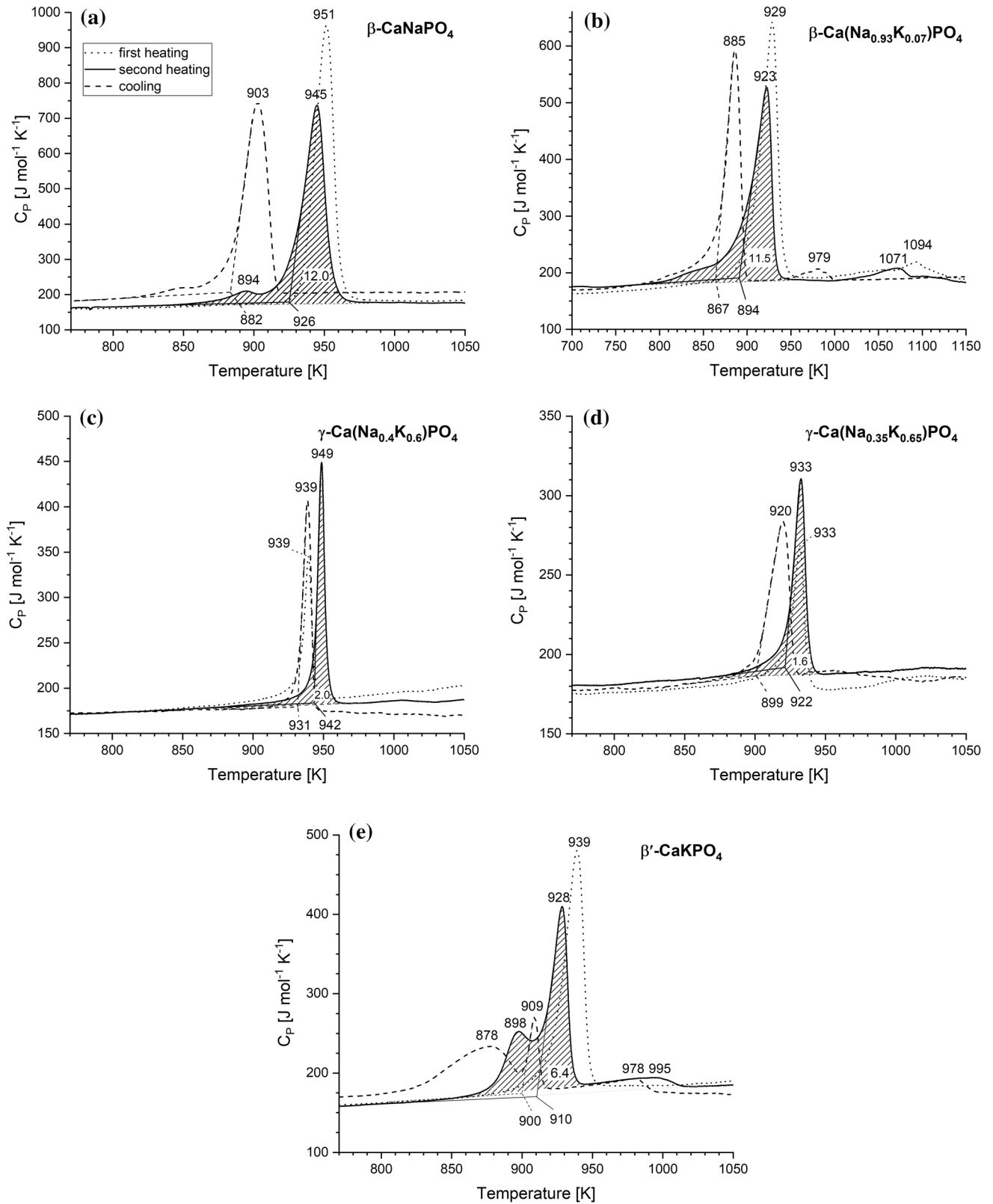
	Na-phase		Na-rich		Intermediate		K-phase	
	CaNaPO_4	$\beta\text{-CaNaPO}_4$	$\beta\text{-Ca}(\text{Na}_{0.93}\text{K}_{0.07})\text{PO}_4$	$\gamma\text{-Ca}(\text{Na}_{0.4}\text{K}_{0.6})\text{PO}_4$	$\gamma\text{-Ca}(\text{Na}_{0.35}\text{K}_{0.65})\text{PO}_4$	$\beta'\text{-CaKPO}_4$		
$\Delta_{\text{diss}}H$ in 5 N HCl	–	$-52.23^a \pm 0.30^b(7)^c$	$-53.25 \pm 0.23(6)$	$-60.90 \pm 0.15(6)$	$-61.69 \pm 0.10(6)$	$-62.69 \pm 0.14(6)$		
$\Delta_f H^\circ$	-2032.7	-2018.3 ± 2.2	-2019 ± 2.4	-2022.1 ± 2.4	-2023.5 ± 2.4	-2030.5 ± 2.1		
S°	128.7	137.2 ± 1.0	138.5 ± 1.0	145.4 ± 1.0	145.8 ± 1.0	148.6 ± 1.0		
$\Delta_f S^{\text{sd}}$	-417.1	-408.6 ± 1.1	-408.2 ± 1.0	-408.2 ± 1.1	-408.5 ± 1.1	-410.4 ± 1.1		
$\Delta_f G^\circ$	-1908.4	-1896.5 ± 2.4	-1897.3 ± 2.6	-1900.4 ± 2.6	-1901.7 ± 2.6	-1908.1 ± 2.4		

^aMean

^bTwo standard deviations of the mean

^cNumber of measurement

^dCalculated with standard entropies of elements from Robie and Hemingway [33]



◀ **Figure 5** Phase transition region for (a) β -CaNaPO₄, (b) β -Ca(Na_{0.93}K_{0.07})PO₄, (c) γ -Ca(Na_{0.4}K_{0.6})PO₄, (d) γ -Ca(Na_{0.35}K_{0.65})PO₄ and (e) β' -CaKPO₄. The dotted line is for first heating, the solid curve for second heating and dashed line for cooling. The shaded area is the area used for calculation of the transition enthalpy [kJ mol⁻¹] which value is displayed. T onset [K] stands below graphs and T peak [K] above graphs.

Superambient heat capacity measurements

Heat capacity (C_p) measurements using the DSC method were done between 259 and 640 K for sample β -CaNaPO₄ and between 282 and 464 K for the other samples. The agreement between PPMS (2–303 K) and DSC data is very good. The differences at 295 K were < 0.3% for all samples. Additionally, semiquantitative C_p measurements (named as STA) between 310 and 1370 K were done with a Netzsch STA thermoanalytical system. The latter data were used for the characterization of the phase transitions (between 850 and 1000 K for the studied phases) and only used up to 640 K for fitting C_p 's for β -Ca(Na_{0.93}K_{0.07})PO₄ and β' -CaKPO₄. Phase transition temperatures depend on chemical composition and show a hysteresis during heating and cooling cycles (Fig. 5).

Phase transition

The phase transitions for β -CaNaPO₄ and β -Ca(Na_{0.93}K_{0.07})PO₄ take place in two steps [13]. She reported that the low-temperature phase β -CaNaPO₄ and high-temperature α -CaNaPO₄ coexist between 883 K and 933 K. In contrast, Orlov et al. [12] postulated only one transition at T around 950 K.

Experimental C_p data for β -CaNaPO₄ show anomalies at 894 K and 945 K (Fig. 5a). The temperature difference between the two anomalies (50 K) and T onset of 926 K for the second peak correlates well with the data of Znamierowska [13] (Fig. 1). The temperature onset of 894 K for β -Ca(Na_{0.93}K_{0.07})PO₄ is 30 K below the onset temperature for β -CaNaPO₄. The data for β -Ca(Na_{0.93}K_{0.07})PO₄ show an additional small peak at $T = 1071$ K which can be explained neither by the existing phase diagrams nor a pyrophosphate impurity (Fig. 5b).

γ -Ca(Na_{0.4}K_{0.6})PO₄ and γ -Ca(Na_{0.35}K_{0.65})PO₄ have each a single C_p anomaly, in agreement with the phase diagram. The temperature onset for sample γ -

Ca(Na_{0.35}K_{0.65})PO₄ is 20 K below that for γ -Ca(Na_{0.4}K_{0.6})PO₄ (Fig. 5c, d), although the phase diagram suggests that the difference should be only 10 K [13].

The potassium endmember β' -CaKPO₄ transforms also in two steps with peak temperatures of 898 K and 928 K and onset temperature of 910 K for the second peak (Fig. 5e). Comparable data are reported by Znamierowska [13] (Fig. 1). Additionally, a broad C_p anomaly is observed in the temperature interval 950–1010 K.

Enthalpy and entropy of phase transition

Data for enthalpy and entropy of phase transition are listed in Table 4. The enthalpy of phase transition of the intermediate phases γ -Ca(Na_{0.4}K_{0.6})PO₄ and γ -Ca(Na_{0.35}K_{0.65})PO₄ is smaller compared to other phases, because both low- and high- temperature phases of the intermediate samples are structurally related [14]. The more complex change from orthorhombic (β -CaNaPO₄, β -Ca(Na_{0.93}K_{0.07})PO₄) and monoclinic (β' -CaKPO₄) to hexagonal symmetry results in higher enthalpy values. The transition enthalpies of the intermediate phases are comparable to the transition enthalpy of Ca(Na_{0.4}K_{0.6})PO₄ reported by Orlov et al. [12] but lower enthalpies are reported for β -CaNaPO₄ and β' -CaKPO₄. Calculated transition enthalpies ($\Delta_{\text{trs}}H$) and entropies ($\Delta_{\text{trs}}S$) in Table 4 are considered in the thermodynamic functions for β -CaNaPO₄ at the onset temperature (Table 6).

Determination of superambient heat capacity

For the high-temperature regions, the DSC data were combined with STA data and estimate for the highest temperature (1400 K). In the region of 640–1400 K, phase transitions of the studied phosphates precluded accurate and precise C_p determination. The function used by Berman and Brown [34] was selected to allow for extrapolation to $T = 1400$ K.

$$C_p(T) = A_0 + A_1 \times T^{-0.5} + A_2 \times T^{-2} + A_3 \times T^{-3}$$

The procedure chosen here agrees with the way the data in the FactSage database were derived, where the data were adjusted to reproduce the main features of the known phase diagrams. We acknowledge that there should be separate C_p functions for the low- and high-temperature phases but the data

Table 4 Thermodynamic properties of the phase transformations. T^{trs} is onset temperature of phase transition

	Na-rich		Intermediate		K-phase
	β -CaNaPO ₄	β -Ca(Na _{0.93} K _{0.07})PO ₄	γ -Ca(Na _{0.4} K _{0.6})PO ₄	γ -Ca(Na _{0.35} K _{0.65})PO ₄	β' -CaKPO ₄
T^{trs} [K]	926 K	894 K	942 K	922 K	910 K
$\Delta_{\text{trs}}H$ [kJ mol ⁻¹]	12.0	11.5	2.0	1.6	6.4
$\Delta_{\text{trs}}S$ [J mol ⁻¹]	13.0	12.9	2.1	1.7	7.0

available do not allow for fitting in such a detail. Instead, just as practiced in FactSage, a single function is proposed. Given that these structures are closely related, and the transitions are only displacive in their nature, such treatment may be deemed acceptable. For calculating one single function, we force the extrapolation to a fixed point at $T = 1400$ K and $C_p = 182.5$ J mol⁻¹ K⁻¹, a value higher than the Dulong–Petit limit of 174.6 J mol⁻¹ K⁻¹, in agreement with the FactSage approach, and STA data for β -CaNaPO₄ and β' -CaKPO₄. Coefficients of all fits are summarized in Table 5.

Heat capacities were fitted well in the temperature ranges from 260 to 640 K for sample β -CaNaPO₄ and from 280 to 640 K for β -Ca(Na_{0.93}K_{0.07})PO₄ and β' -CaKPO₄. These were extrapolated to 1400 K for these three samples (Fig. 6a, b, d, Table 5). In the measured range for β -CaNaPO₄, our data are consistently lower than those listed in FactSage (Fig. 6a). An explanation of the difference is difficult because it is not clear if the FactSage data are based on measurements or estimates. Furthermore, the values for the thermodynamic functions, calculated from the fit polynomials, are reported for β -CaNaPO₄ in Table 6.

Measurements for the intermediate compositions γ -Ca(Na_{0.4}K_{0.6})PO₄ and γ -Ca(Na_{0.35}K_{0.65})PO₄ compositions show a similar C_p increase between 380 and 460 K. Fitting was impeded due to the β' to γ -phase transition between 480 to 580 K (Fig. 6c), also displayed in phase diagram (Fig. 1).

The heat capacity for β' -CaKPO₄ was fitted between 280 and 640 K. The extrapolated C_p values also fixed at 182.5 J mol⁻¹ K⁻¹, differ strongly from the semiquantitative C_p measurements between 1000 and 1400 K (Fig. 6d).

Table 5 Heat capacities for the studied phases, fitted to polynomials $C_p(T) = A_0 + A_1 \cdot T^{-0.5} + A_2 \cdot T^{-2} + A_3 \cdot T^{-3}$ [34]. These polynomial-coefficients were determined between 260 and 640 K (DSC data) for sample β -CaNaPO₄; between 280 and 640 K (DSC/STA data) for samples β -Ca(Na_{0.93}K_{0.07})PO₄ and β' -CaKPO₄; and a fixed $C_p = 182.5$ J·mol⁻¹ K⁻¹ at $T = 1400$ K

Phase	β -CaNaPO ₄	β -Ca(Na _{0.93} K _{0.07})PO ₄	β' -CaKPO ₄
A_0	199.92	189.60	211.36
A_1	- 496.08	- 32.064	- 1047.5
A_2	- 8.0376·10 ⁶	- 1.1879·10 ⁷	- 3.0740·10 ⁶
A_3	1.2116·10 ⁹	1.9318·10 ⁹	3.1578·10 ⁸

Conclusion

Thermodynamic properties of technically important calcium alkali phosphates Ca(Na,K)PO₄ have been determined by different calorimetric measurements. Based on these data, standard enthalpies of formation and standard entropies were calculated for the low-temperature phases β -CaNaPO₄, β -Ca(Na_{0.93}K_{0.07})PO₄, γ -Ca(Na_{0.4}K_{0.6})PO₄, γ -Ca(Na_{0.35}K_{0.65})PO₄ and β' -CaKPO₄. Besides, the sodium endmember all samples contain apatite, whitlockite, or pyrophosphate as impurities. All thermodynamic data were corrected for these impurities. The deviation is < 1% for standard entropy and < 0.1% for standard enthalpy of formation in case experimental values are compared with corrected ones.

The phase transformations from low- to high-temperature phases took place in the temperature range 890 K to 950 K which agrees with the phase diagram reported by Znamierowska [13]. Additionally observed heat capacity anomalies could not be

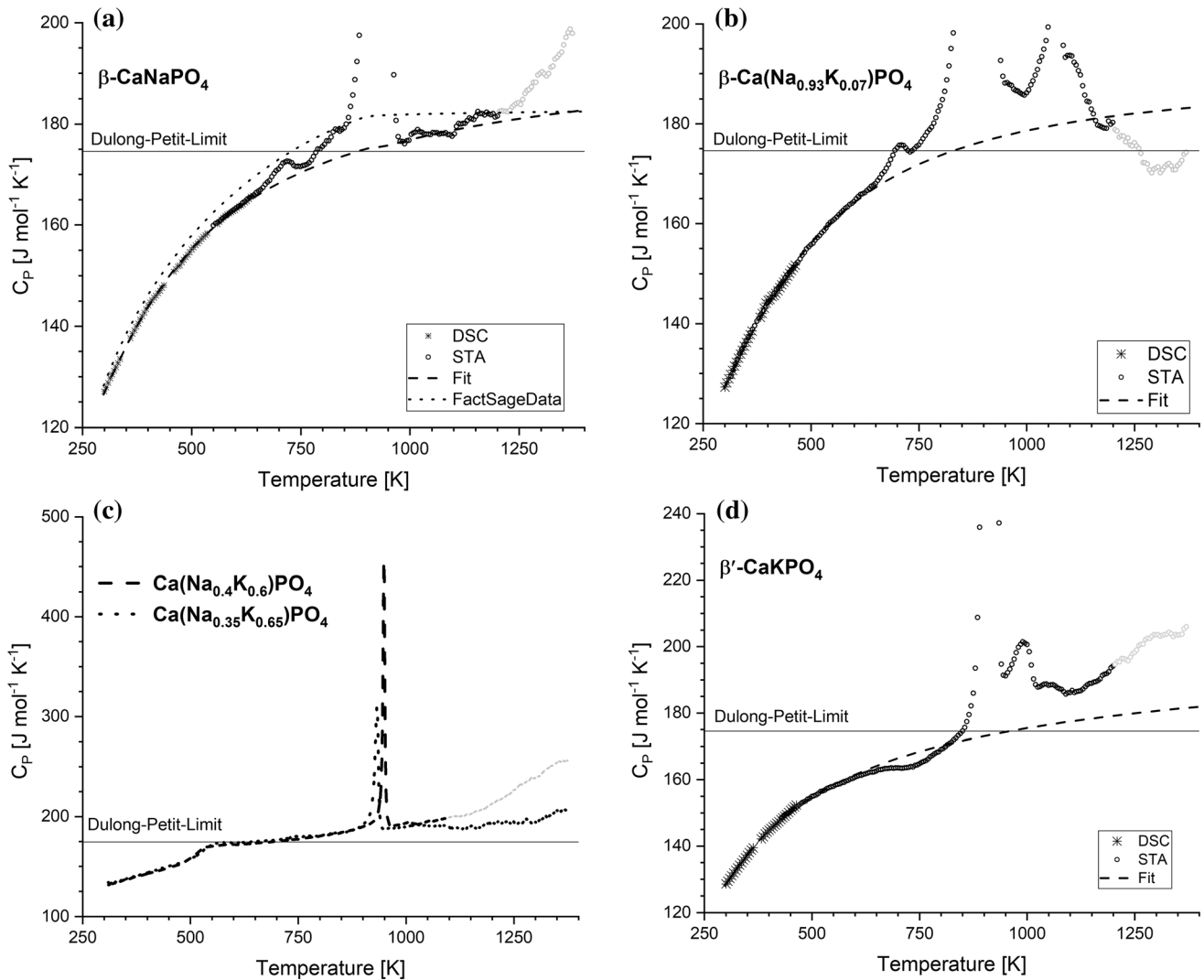


Figure 6 Data (series DSC and STA) and fits of heat capacity for (a) β -CaNaPO₄, (b) β -Ca(Na_{0.93}K_{0.07})PO₄, (c) γ -Ca(Na_{0.4}K_{0.6})PO₄ and γ -Ca(Na_{0.35}K_{0.65})PO₄ and (d) β' -CaKPO₄. The curve “FactSageData” in (a) was calculated from entries in the

database of the software FactSage. C_p anomaly between 480 and 580 K in c) is the β' -to- γ phase transition (Fig. 1). Light grey circles of STA represent values with low accuracy above 1100 K.

matched to phase transition reactions of calcium alkali phosphates or any impurities. Further investigations are required to interpret these anomalies.

Heat capacity measurements at superambient temperatures were challenging because of phase transitions and low accuracy of the used high-temperature calorimetric method. Thus, heat capacities between 640 and 1400 K were estimated by

extrapolation for samples β -CaNaPO₄, β -Ca(Na_{0.93}K_{0.07})PO₄ and β' -CaKPO₄.

In summary, the determined thermodynamic properties of Ca(Na,K)PO₄ are valuable data for thermodynamic calculations that can improve manufacturing bioceramics and the production of phosphorus fertilizers containing these calcium alkali phosphates.

Table 6 Thermodynamic functions for β -CaNaPO₄ ($M_r = 158.04 \text{ g mol}^{-1}$). Data for phase transition at 926 K are listed in Table 5

T K	C_p $\text{J mol}^{-1} \text{ K}^{-1}$	S° $\text{J mol}^{-1} \text{ K}^{-1}$	$[H(T) - H(0)]/T$ $\text{J mol}^{-1} \text{ K}^{-1}$	$- [G(T) - H(0)]/T$ $\text{J mol}^{-1} \text{ K}^{-1}$
0	0	0		
10	0.15	0.05	0.03	0.01
20	1.75	0.50	0.39	0.11
30	5.90	1.89	1.45	0.44
40	12.66	4.46	3.36	1.10
50	20.77	8.13	6.02	2.12
60	29.38	12.68	9.19	3.48
70	37.74	17.84	12.68	5.16
80	45.42	23.39	16.30	7.09
90	52.46	29.14	19.92	9.22
100	59.27	35.03	23.52	11.50
120	70.75	46.90	30.48	16.41
140	80.48	58.56	36.95	21.61
160	88.74	69.85	42.91	26.94
180	96.29	80.75	48.44	32.31
200	102.61	91.23	53.54	37.69
220	108.47	101.3	58.27	43.02
240	113.68	110.0	62.68	48.28
260	118.46	120.3	66.79	53.46
273.15	121.68	126.2	69.35	56.82
280	123.28	129.2	70.65	58.55
298.15	126.75	137.1	73.96	63.09
300	126.84	138.0	74.31	63.71
350	136.05	161.5	84.45	77.01
400	143.81	182.7	93.00	89.72
450	150.14	202.2	100.35	101.82
500	155.27	220.1	106.73	113.33
550	159.48	236.6	112.33	124.29
600	162.95	252.0	117.27	134.73
650	165.85	266.3	121.66	144.69
700	168.30	279.8	125.59	154.20
750	170.38	292.4	129.12	163.31
800	172.18	304.3	132.31	172.03
850	173.75	315.6	135.21	180.40
900	175.12	326.3	137.86	188.45
926	175.77	331.7	139.14	192.51
Phase transition $\beta \rightarrow \alpha$				
926	175.77	344.6	152.10	192.51
950	176.33	349.4	152.91	196.52
1000	177.40	359.1	154.51	204.60
1100	179.23	377.2	157.37	219.83
1200	180.71	393.8	159.87	233.95
1300	181.95	409.2	162.06	247.12
1400	183.00	423.5	164.00	259.45

Acknowledgements

Open Access funding provided by Projekt DEAL. The research was done in the framework of the Project ASHES financed by the German Federal Ministry of Education and Research (BMBF, Grant No. 031A288).

Compliance with ethical standards

Conflict of interest The authors declare that they have no conflict of interest.

Electronic supplementary material: The online version of this article (<https://doi.org/10.1007/s10853-020-04615-5>) contains supplementary material, which is available to authorized users.

Open Access This article is licensed under a Creative Commons Attribution 4.0 International License, which permits use, sharing, adaptation, distribution and reproduction in any medium or format, as long as you give appropriate credit to the original author(s) and the source, provide a link to the Creative Commons licence, and indicate if changes were made. The images or other third party material in this article are included in the article's Creative Commons licence, unless indicated otherwise in a credit line to the material. If material is not included in the article's Creative Commons licence and your intended use is not permitted by statutory regulation or exceeds the permitted use, you will need to obtain permission directly from the copyright holder. To view a copy of this licence, visit <http://creativecommons.org/licenses/by/4.0/>.

References

- [1] Orlov NK, Putlayev VI, Evdokimov PV, Safronova TV, Klimashina ES, Milkin PA (2018) Resorption of $\text{Ca}_{3-x}\text{M}_{2x}(\text{PO}_4)_2$ (M = Na, K) calcium phosphate bioceramics in model solutions. *Inorg Mater* 54(5):500–508
- [2] Berger G, Gildenhaar R, Ploska U (1995) Rapid resorbable, glassy crystalline materials on the basis of calcium alkali orthophosphates. *Biomaterials* 16(16):1241–1248
- [3] Evdokimov PV, Putlayev VI, Ivanov VK, Garshev AP, Shatalova TB, Orlov NK, Klimashina ES, Safronova TV (2014) Phase equilibria in the tricalcium phosphate-mixed calcium sodium (potassium) phosphate systems. *Russ J Inorg Chem* 59(11):1219–1227
- [4] Gunawardane RP, Glasser FP (1979) Reaction of chlorapatite, $\text{Ca}_5(\text{PO}_4)_3(\text{Cl}, \text{F})$ with sodium carbonate and silica. *J Mater Sci* 14:2797–2810. <https://doi.org/10.1007/BF00611458>
- [5] Herzel H, Krüger O, Hermann L, Adam C (2016) Sewage sludge ash : a promising secondary phosphorus source for fertilizer production. *Sci Total Environ Part B* 542:1136–1143
- [6] Messerschmitt A (1938) Die Aufschließung der Rohphosphate durch Sintern mit Alkalisilicat. *Angew Chem* 51(14):197–203
- [7] Franck HH, Bredig MA, Frank R (1936) Untersuchungen über Kalk-Alkaliphosphate. I. Ein Beitrag zur Kenntnis des Rhenaniaphosphates. *Z Anorg Allg Chem* 230:1–27
- [8] Watti A, Alnjar M, Hammal A (2016) Improving the specifications of Syrian raw phosphate by thermal treatment. *Arab J Chem* 9:S637–S642
- [9] Nakamura S, Kanda T, Imai T, Sawadogo J, Nagumo F (2019) Solubility and application effects of African low-grade phosphate rock calcinated with potassium carbonate. *Soil Sci Plant Nutr* 65(3):267–273
- [10] Stemann J, Peplinski B, Adam C (2015) Thermochemical treatment of sewage sludge ash with sodium salt additives for phosphorus fertilizer production—analysis of underlying chemical reactions. *Waste Manag* 45:385–390
- [11] Steckenmesser D, Vogel C, Adam C, Steffens D (2017) Effect of various types of thermochemical processing of sewage sludges on phosphorus speciation, solubility, and fertilization performance. *Waste Manag* 62:194–203
- [12] Orlov NK, Evdokimov PV, Milkin PA, Garshev AV, Putlayev VI, Grebenev VV, Günster J (2019) Phase equilibria in $\text{CaNaPO}_4\text{--CaKPO}_4$ system and their influence on formation of bioceramics based on mixed Ca–K–Na phosphates. *J Eur Ceram Soc* 39(16):5410–5422
- [13] Znamierowska T (1982) Uklad $\text{Ca}_3(\text{PO}_4)_2\text{--CaNaPO}_4\text{--CaKPO}_4$. *Zesz Nauk Politech Slask Ser* 709(100):35–56
- [14] Schneider M, Gildenhaar R, Berger G (1994) Investigations of phase relations in the system $\text{CaO}*\text{Na}_2\text{O}*\text{K}_2\text{O}*\text{P}_2\text{O}_5$. *Cryst Res Technol* 29(5):671–675
- [15] Jinlong N, Zhenxi Z, Dazong J (2003) Structure determination of $\text{Ca}_2\text{KNa}(\text{PO}_4)_2$ with wide-angle XRD. *Rare Met Mater Eng* 3(2):173–175
- [16] Ben Amara M, Vlasse M, Le Flem G, Hagenmuller P (1983) Structure of the low-temperature variety of calcium sodium orthophosphate, NaCaPO_4 . *Acta Crystallogr Sect C* 39(11):1483–1485
- [17] Ando J, Matsuno S (1968) $\text{Ca}_3(\text{PO}_4)_2\text{--CaNaPO}_4$ System. *B Chem Soc Jpn* 41(2):342–347
- [18] Bredig MA (1942) Isomorphism and allotropy in compounds of the type A_2XO_4 . *J Phys Chem-U.S.* 46(6):747–764

- [19] Wanmaker WL, Spier HL (1962) Luminescence of copper-activated orthophosphates of the type $ABPO_4$ ($A = Ca, Sr,$ or Ba and $B = Li, Na,$ or K). *J Electrochem Soc* 109(2):109–114
- [20] Zdukos AT, Beglow BM, Chaimow BM (1971) Calculation of the enthalpies of calcium pyrophosphates. *Uzb Khim Zh* 15:21–24
- [21] Morris MC, McMurdie HF, Evans EH, Paretzkin B, de Groot JH, Weeks BS, Newberry RJ (1978) Standard X-ray diffraction powder patterns: section 15. Data for 112 substances. *Natl Bur Stand* 25(15):69
- [22] Franck HH, Bredig MA, Kanert E (1938) Untersuchungen über Kalk-Alkaliphosphate. II. Über Calciu-Kalium-Phosphate. *Z Anorg Allg Chem* 237:49–78
- [23] Majzlan J (2017) Solution calorimetry on minerals related to acid mine drainage—methodology, checks, and balances. *Acta Geol Slovaca* 9:171–183
- [24] Parker VB (1965) Thermal properties of uni-univalent electrolytes. National standard reference data series, vol 2. National Bureau of Standards, Gaithersburg
- [25] Kennedy CA, Stancescu M, Marriott RA, White MA (2007) Recommendations for accurate heat capacity measurements using a quantum design physical property measurement system. *Cryogenics* 47(2):107–112
- [26] Benisek A, Kroll H, Dachs E (2012) The heat capacity of fayalite at high temperatures. *Am Miner* 97(4):657–660
- [27] Hemingway BS (1987) Quartz: heat capacities from 340 to 1000 K and revised values for the thermodynamic properties. *Am Miner* 72(3–4):273–279
- [28] Chai L, Navrotsky A (1996) Synthesis, characterization, and enthalpy of mixing of the $(Fe, Mg)CO_3$ solid solution. *Geochim Cosmochim Acta* 60(22):4377–4383
- [29] Majzlan J (2011) Thermodynamic stabilization of hydrous ferric oxide by adsorption of phosphate and arsenate. *Environ Sci Technol* 45(11):4726–4732
- [30] Rud'ko PK, Yaglov VN, Novikov GI (1974) Thermodynamic characteristics of some potassium phosphates. *Obshchaya i Prikladnaya Khimiya* 6:9–11
- [31] Wagman DD (1982) The NBS tables of chemical thermodynamic properties : selected values for inorganic and C1 and C2 organic substances in SI units. National Bureau of Standards, Washington
- [32] Luff BB, Reed RB (1978) Standard enthalpies of formation of monopotassium and dipotassium orthophosphate. *J Chem Eng Data* 23(1):60–62
- [33] Robie RA, Hemingway BS (1995) Thermodynamic properties of minerals and related substances at 298.15 K and 1 bar (10^5 pascals) pressure and at higher temperatures. U.S. Geol Surv Bull. <https://doi.org/10.3133/b2131>
- [34] Berman RG, Brown TH (1985) Heat capacity of minerals in the system $Na_2O-K_2O-CaO-MgO-FeO-Fe_2O_3-Al_2O_3-SiO_2-TiO_2-H_2O-CO_2$: representation, estimation, and high temperature extrapolation. *Contrib Miner Petrol* 89(2):168–183
- [35] Bale CW, Bèlisle E, Chartrand P, Decterov SA, Eriksson G, Gheribi AE, Hack K, Jung IH, Kang YB, Melançon J, Pelton AD, Petersen S, Robelin C, Sangster J, Spencer P, Van Ende MA (2016) FactSage thermochemical software and databases, 2010–2016. *Calphad* 54:35–53

Publisher's Note Springer Nature remains neutral with regard to jurisdictional claims in published maps and institutional affiliations.